Advances in Engineering Research, volume 188

International Conference on Aviamechanical Engineering and Transport (AviaENT 2019)

Feasibility Study of Ultrasonic De-Icing Technique for Aircraft Wing Ice Protection

Vladislav Daniliuk
School of Aeronautic Science and Engineering
Beihang University
Beijing, China
vlad.mai@mail.ru

Evgeny Pamfilov
Research Laboratory of Materials Engineering and Adaptive Technological Systems
Bryansk State Technical University
Bryansk, Russia
epamfilov@yandex.ru

Aleksey Daniliuk
Research Laboratory of Materials Engineering and Adaptive Technological Systems
Bryansk State Technical University
Bryansk, Russia

Yuanming Xu
School of Aeronautic Science and Engineering
Beihang University
Beijing, China

***Abstract*—Flight in icing conditions brings significant safety risks due to aircraft aerodynamic performance reduction, stability and controllability deterioration, failures, mechanical damages. For reliable operation in icing conditions active anti-icing/de-icing systems are needed, which entail at the present time considerable on-board power consumption, additional weight, installation or maintenance difficulties and other drawbacks. Moreover, a lot of incidents still appear due to in-flight icing. Nowadays, it is a high demand for efficient and reliable de-icing techniques. Recent studies presented hybrid and non-thermal in-flight ice protection methods with potentials to be more advantageous, including ultrasonic de-icing technique. In this paper, the feasibility study with semi-hard lead zirconate titanate (PZT) ultrasonic Langevin-type transducer was carried out. The theoretical model explaining ice detaching mechanism with applied ultrasonic guided wave propagation theory was described. The verifying experiment was conducted to prove feasibility of de-icing. Prospects for further research were given.**

Keywords—aircraft wing de-icing; ultrasonic de-icing; ice protection system; piezoelectric transducer

I. INTRODUCTION

The experience of the aircraft operation shows that in-flight icing along with atmospheric turbulence, electrical discharges, collision with birds, - is one of the most dangerous effects of the natural environment, which significantly affects on flight safety More than a thousand deaths and hundreds of accidents over the past three decades occurred due to the problem of icing [1]. Supercooled clouds cause the majority of aircraft icing events. In these clouds the air temperature is below 0 °C. In aviation, according to the Federal Aviation Regulations Part 23, Part 25 (FAR-23, FAR-25 Appendix C) [2], the aircraft icing intensity level depends on three variables: the liquid water content (LWC), the ambient air temperature, and the MVD or the Mean Effective Diameter (MED) for estimated water droplet distribution calculations.

Icing of an aircraft wing increases drag and reduces lift, stall angle of attack and, therefore, engine thrust. As a consequence, the aerodynamic performance of an aircraft significantly decreased. It negatively affects on aircraft stability and controllability.

The level of the performance deterioration can be very high. In icing conditions, the maximum lift coefficient of NACA 65A413 airfoil is reduced by nearly 50%, the stall angle of attack is reduced by 6° [3]. The drag of a wing in icing conditions is increasing by about 50% and the maximum value can reach 200% [4,5,6].

The variety of active ice protection systems is proposed for safe operation of an aircraft. However, the power consumption values are very high for the most common ice protection systems which are thermal. It was reported that consumed power density can reach up to 62 kW/m^2 for electro-resistive anti-/de-icing system [7]. Hot air systems, lead to a loss of power (thrust) from 10 to 15% for a turboprop engine [8]. Nevertheless, the energy efficiency and fuel consumption are essential for aviation.

The mechanical and thermo-mechanical methods were considered in recent studies as the most promising energy-saving de-icing techniques for an aircraft wing. In these studies, ultrasonic guided wave de-icing technique is expected to improve energy efficiency and exclude thermal impact on protected surfaces as well as runback ice accretions. However, recent research does not provide for this technique a comprehensive methodology of piezoelectric materials and transducers selection. In this paper, the feasibility study of Langevin-type PZT transducer application for de-icing of the aluminium plate, imitating the aircraft airfoil leading edge skin is carried out. The simulation defining optimal ultrasonic frequency and ice-plate shear stress values is presented. The theoretical approach of this de-icing method is also described.

II. THEORETICAL MODEL OF ULTRASONIC DE-ICING TECHNIQUE

The idea of ultrasonic method is based on the fact that the adhesion shear forces between ice and surface of the aircraft skin are relatively small. Therefore, ice layer can be easily delaminated by applying shear stress at the interface of skin material. To achieve de-icing effect, the stress must exceed the adhesion shear strength of the ice layer. The generation of the shear stress over the layered ice-surface structure can be initiated by propagation of ultrasonic waves that are induced by piezoelectric actuators.

The simplified model has been proposed for evaluation of the de-icing effect. Similar to the iced aircraft airfoil skin, the physical model is assumed to be an aluminium plate covered by the ice layer.

The interface and bulk ultrasonic waves are generated in the airfoil skin by attached piezoelectric transducers. In order to calculate the interface shear stress values produced from these waves, the elastic wave propagation theory is applied. According to this theory, the waves propagating in the infinite plate can appear in the various combinations. De-icing of the plate in established model is assumed by the group of the ultrasonic guided waves: Lamb waves and horizontal shear waves (SH waves). Lamb waves are characterized as the waves with polarization along the x_3 axis (vertical polarization). SH waves are the elastic transverse waves with polarization along the x_2 axis (horizontal polarization), as it is shown on Fig. 1 [9].

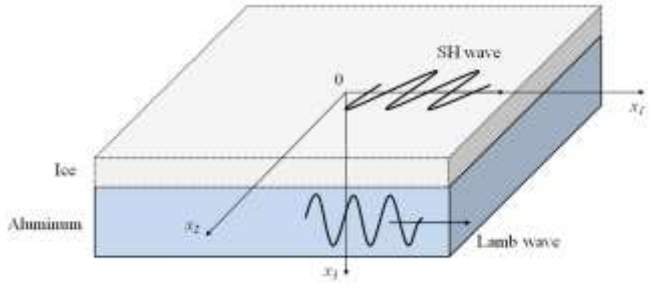

Fig. 1. The scheme of Lamb and SH wave propagation in iced plateption.

Depending on the ultrasonic frequency, bonding parameters, material density, and the plate thickness, the surface or interface waves, such as Love, Stonely or Rayleigh waves may appear [10,11]. These waves were omitted in the current study due to the chosen range of ultrasonic frequencies.

A. Ultrasonic guided wave propagation theory

To predict the interface shear stresses and displacements, caused by the ultrasonic guided waves in structure, the following governing equation for waves in solid media is employed

$$\rho \frac{\partial^2 u_i}{\partial t^2} = c_{ijkl} \frac{\partial^2 u_i}{\partial x_j \partial x_k} \tag{1}$$

where ρ is the material's density, C_{ijkl} is the stiffness matrix, and u_i is the displacement field.

The general trial solution for (1) as follows:

$$u_i = U_i e^{ik(x_1 + \alpha x_3 - ct)} \tag{2}$$

where, U_i is the polarization vector that represents the displacement vector in each direction, k is the wave number along x_1 direction, c is the phase velocity along x_1 direction, and α is the ratio of wave number in x_3 direction with respect to the wave number in the x_1 direction.

Lamb waves polarized along x_1 and x_3 directions, therefore polarization vector U_2 is equal to zero. The displacements and stresses are obtained by Christoffel's equation as u_1 and u_3:

$$u_1 = \sum_{k=1}^{4} B_k e^{ik(x_1 + \alpha_k x_3 - ct)} \tag{3}$$

$$u_3 = \sum_{k=1}^{4} B_k U_{3k} e^{ik(x_1 + \alpha_k x_3 - ct)} \tag{4}$$

$$\sigma_{31} = \sum_{k=1}^{4} B_k [\alpha_k + U_{3k}] \mu (ik) e^{ik(x_1 + \alpha_k x_3 - ct)} \tag{5}$$

$$\sigma_{32} = \sum_{k=1}^{4} B_k [\lambda + (\lambda + 2\mu)\alpha_k U_{3k}] \mu (ik) e^{ik(x_1 + \alpha_k x_3 - ct)} \tag{6}$$

where U_{3k} is the ratio between the polarization vectors U_3 and U_1; B_k are the weighting coefficients of the partial waves.

Similarly, polarization of SH waves is along x_2 direction, therefore the polarization vectors U_1 and U_3 are taken equal to zero. The displacement and stress induced by SH waves are defined.

$$u_2 = \sum_{j=1}^{2} v_j e^{ik(x_1 + \alpha_j x_3 - ct)} \tag{7}$$

$$\tau_{32} = 2 \sum_{j=1}^{2} v_j \alpha_j \mu (ik) e^{ik(x_1 + \alpha_j x_3 - ct)} \tag{8}$$

where v_j are the weighting coefficients of partial waves.

These equations contain the wave number and the phase velocity. Therefore, the values of displacements and stress can be obtained for defined ultrasonic frequency and material parameters. These solutions are commonly presented by so-called dispersion curves of Lamb and SH waves, which show the relationship between the frequency - plate thickness product and ultrasphase velocity.

The dispersion relations governing symmetric (S) and antisymmetric (A) modes of Lamb and SH waves were obtained by semi-analytical finite element method software (GUIGUW). The dispersion curves of these ultrasonic guided waves for established model are shown for the iced plate specimen in Fig. 2.

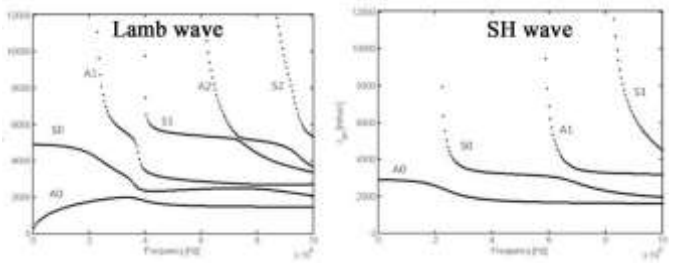

Fig. 2. The scheme of Lamb and SH wave propagation in iced plateption.

The selection of optimal ultrasonic de-icing frequency and the stress propagation behaviour can be estimated by the analysis of these dispersion curves. Accordingly, it is expected that the interface shear stress in the iced plate model can reach the maximum values when the ultrasonic frequency range corresponds to the appearance of A_0 and S_0 modes of Lamb and SH waves. Therefore, the initial frequencies should be chosen below 100 kHz.

B. Piezoelectric eguations

The electromechanical coupling problem for piezoelectric materials simulation is defined under moderate electrical field values by the piezoelectric constitutive equations in (9):

$$\begin{cases} T_i = c_{ij}^E S_j + d_{mi} E_m & (i, j = 1,2,3\cdots 6) \\ D_m = d_{mi} S_j + \varepsilon_{mk}^s E_k & (m,k = 1,2,3) \end{cases} \tag{9}$$

where S_j and T_i are the mechanical stress and strain; c_{ij}^E is an elastic stiffness coefficient when electrical displacement is constant; d_{mi} is piezoelectric strain constant; E_m is applied electrical field (V/m); D_m is the polarization (electrical displacement) (C/m^2); ε is the material dielectric permittivity (at zero stress) [41,42]. Piezoelectric strain constant d is the piezoelectric material property value, showing the magnitude of the induced strain by an external electric field

By taking piezoelectric constitutive equations into consideration, the finite element matrix equation for harmonic analysis of piezoelectric transducer with iced plate assembly is defined in (10).

$$\begin{bmatrix} K_{uu} - \omega^2 M & K_{u\varphi} \\ K_{u\varphi} & K_{\varphi\varphi} \end{bmatrix} \begin{bmatrix} U \\ \Phi \end{bmatrix} = \begin{bmatrix} 0 \\ -Q \end{bmatrix} \tag{10}$$

where K_{uu} is the elastic stiffness matrix (N/m); ω is the angular frequency; M is the structure mass matrix; $K_{u\phi}$ is the piezoelectric stiffness matrix (N/V); $K_{\phi\phi}$ is the dielectric matrix (F); U is the displacement field; Φ is the electric potential strength; Q is the vector of the nodal charges (C)

III. NUMERICAL SIMULATION

The harmonic resonance analysis was performed in order to obtain the values of the frequencies with the highest level of acoustic wave amplitudes. The finite element method (FEM) harmonic simulations were made through the commercial software (ANSYS). Further the ice-plate interface shear stresses can be calculated.

A. Piezoelectric material parameters

Material parameters of PZT-4 material used in simulation are listed in Table 1 and Table 2:

TABLE I. PZT-4 CONSTANTS

Clamped dielectric constants $\varepsilon_{ii}^S / \varepsilon_0$ (-)			**Piezoelectric stress constant** e (C/m^2)		
ε_{11}^S	ε_{22}^S	ε_{33}^S	e_{15}	e_{31}	e_{33}
748	748	871	11.33	-5.50	15.08

TABLE II. PZT-4 ELASTIC STIFFNESS PARAMETERS

Elastic stiffness constants $c_{ij}(10^{10} N \cdot m^{-2})$					
c_{11}^E	c_{12}^E	c_{13}^E	c_{33}^E	c_{44}^E	c_{66}^E
13.9	7.5	7.8	12.6	2.8	2.1

B. The model of transducer installation

An aluminium plate with geometrical size of 300×210×2 mm and two PZT-4 transducers were adopted for simulations and experiment. The ice layer thickness is 2mm. The density, Young's modulus and Poisson's ratio of the ice at -15 °C, which are 913 kg/m^3, 6 GPa and 0.34 respectively. The distance between transducers was calculated according to the requirement of operation frequency matching as shown in (11).

$$r = (n + \frac{1}{2})\lambda_f, n = 1,2,3\ldots\ldots \tag{11}$$

where r is the distance between transducer centerlines and λ_f is the wavelength of the ultrasonic signal

The adopted PZT-4 transducers are the Langevin-type ultrasonic actuators which are utilizing for power applications. This type of transducers consists from piezoelectric layers stacked between the metal parts, which are also called front mass and damper. The dimensions and shape of entire unit are specifically designed to achieve the highest amplitude of the ultrasonic wave output at the resonant frequencies. The adopted PZT-4 transducer is a conventional Langevin-type actuator with aluminum front mass and stainless steel damper.

The meshed assembled model is shown in Fig. 3. The plate smaller side is clamped for simulation and experiment.

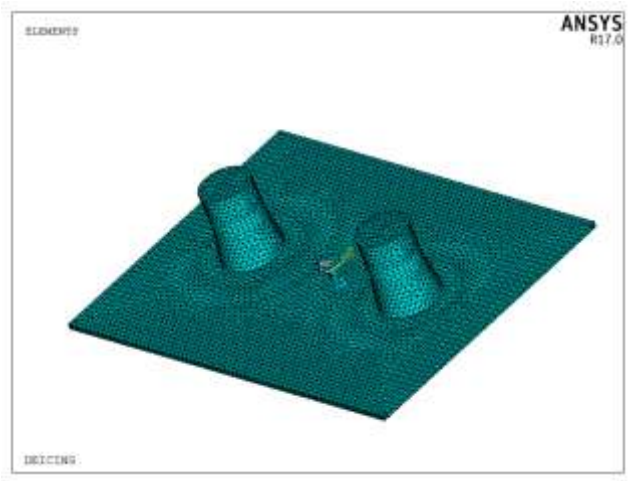

Fig. 3. Meshed finite element model.

C. The optimal ultrasonic frequency

The range of the optimal frequency for the model was determined by using the dispersion curves. Further, several representative nodes were chosen in the model at the ice-material interface in order to determine optimal frequency. The variation of stress with alternating ultrasonic frequency was investigated to find the resonant frequency. Fig. 4 shows the interface stress amplitude - frequency curves of the representative nodes in horizontal plane (x_3 equal to zero).

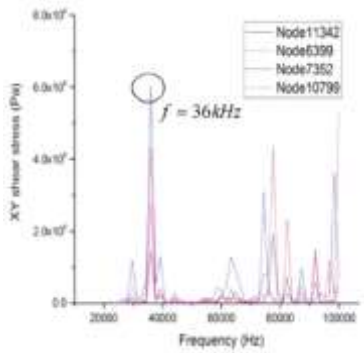

Fig. 4. The interface shear stress amplitude versus frequency for the chosen node.

As it is seen from the graph, the resonating ultrasonic frequency of the iced plate specimen is 36.0 kHz. This frequency is also corresponding to the electro-mechanical resonance frequency of adopted PZT-4 transducers.

D. The interface shear stress analysis

Then, harmonic resonance analysis was carried out for the assembly of piezoelectric transducers, aluminium plate and ice layer. The stress distribution in the structure was defined for these frequencies, as shown in Fig. 5.

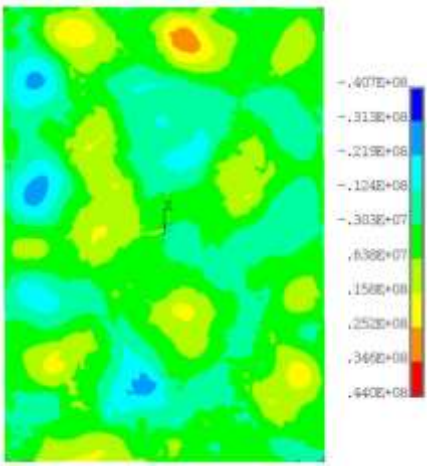

Fig. 5. Interface shear stress distribution.

The ice accretions are delaminated from plate when the interfacial stress between ice and substrate exceeds the adhesive shear strength. The adhesive shear strength between aluminium plate and ice layer at -20°C was adopted from the relevant literature to be 0.35 MPa [12]. According to the simulation, the interface shear stress values are greater than 3.03 MPa in the most area. It means that the ice shedding effect is achieved.

IV. Ultrasonic De-icing Experiment

An experimental installation was built to verify the numerical simulations and feasibility of ice detaching from the plate. This installation contains following parts: ultrasonic frequency generator, amplifier, assembly of ultrasonic transducers on aluminium plate, clamping holder, refrigerator for the ice accretion, measuring and recording instruments, as shown in Fig. 6.

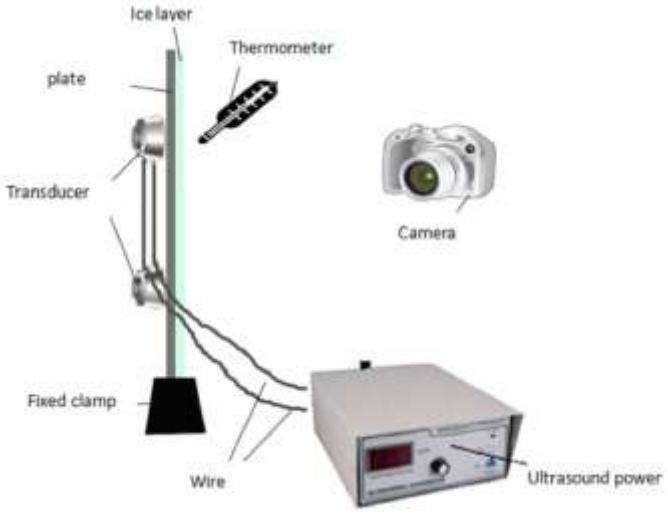

Fig. 6. Schematic diagram with equipment for ultrasonic deicing experiment.

The maximum power output from ultrasonic power generator is 440 W; the frequency can be adjusted continuously from 20 kHz to 150 kHz. The 2mm ice layer was

formed in an environment of -15°C on aluminium plate. Ice layer has been held at −15°C for an hour to reach stronger adhesion with the aluminum plate surface.

The preparation of the entire experiment and the main steps of the experiment are as follow:

1. Polishing aluminium plate
2. Sticking PZT-4 transducers on the plate with epoxy glue
3. Connecting of the wire to the ultrasonic transducers
4. Placing of the plate to the freezer
5. Covering free side of the plate with cold water
6. Connecting of the wire to the ultrasonic amplifier after the ice layer formed
7. Turning on the measuring and recording equipment and starting experiment

In the conducted experiment instantaneous de-icing effect was observed, and after about a minute ice was completely removed, as shown in Fig. 7.

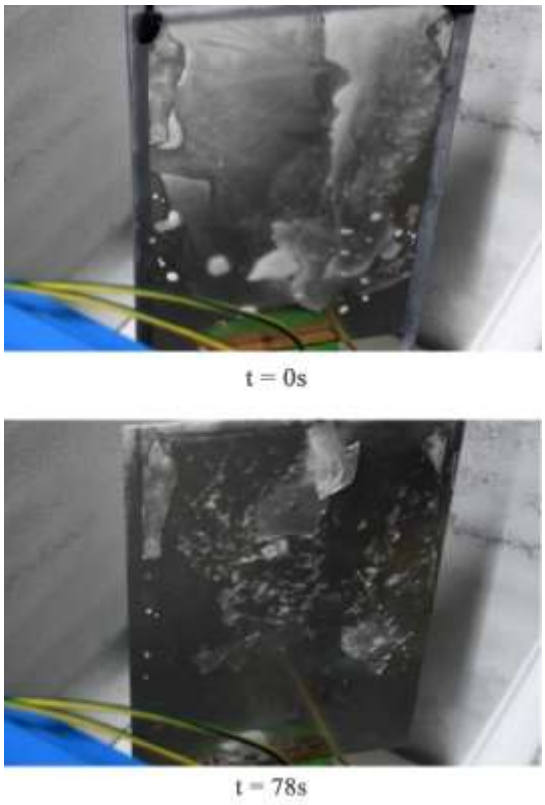

Fig. 7. Crack of the ice at t = 0s and full ice shedding at t = 78s.

The consistency of experimental and simulation results is verified. However, relatively long de-icing time indicates that one of the de-icing reasons is the heating effect, possibly appearing in the structure due to the ultrasonic waves attenuation and dissipation.

V. Discussion and Prospect

The power supply for experiment with PZT-4 transducers was defined as 400 W at the working frequency. The calculated power density of 0.63 W/cm^2 according to the iced plate sizes was obtained. It is almost 10 times less, than for conventional thermal de-icing systems. Moreover, the ice shedding process in ultrasonic de-icing initiates immediately, so the time period of ice shedding is assumed considerably shorter than for thermal de-icing. Thus, considerable energy reduction for de-icing with ultrasonic technique makes this method potentially more advantageous.

However, the inability in conducted experiment to delete the ice layer instantaneously indicates about large energy loss. Besides, the ice shedding was achieved only after a minute of system operation. These facts directly connected to the appearance of the heat in the ice-plate interface, which partially caused ice shedding. Nevertheless, the de-icing feasibility with Langevin-type ultrasonic transducer was found comparable in terms of de-icing time and energy consumption with some other types of transducers from previous studies of ultrasonic de-icing [13]. The possible reasons of large energy losses are can be due to transducer-substrate bond line parameters, acoustic and electromechanical impedance matching. Besides, efficient piezoelectric materials can be further studied to improve efficiency of the method.

According to the previous studies, the ultrasonic guided wave de-icing technique is expected to exclude thermal impact on protected surfaces as well as runback ice accretions. Relatively low weight, low cost and maintenance simplicity are also pointed out. However, some aspects such as system reliability including de-icing time, fatigue damages in protected area, and energy dissipation behavior with full-scale experiments observation still need further research. The ultrasonic method could be researched and adapted for reliable de-icing in real atmospheric icing conditions, especially at low temperatures. The combinations of ultrasonic de-icing technique with passive and active de-icing methods might be a promising solution for future flight vehicle de-icing systems.

VI. Conclusion

Ice protection systems with low power consumption and weight are needed for flight vehicle operation. However, the problem of reliable and efficient ice protection method still exists in aviation. In the presented study, power-efficient, non-thermal ultrasonic de-icing method with Langevin-type ultrasonic actuators for aircraft airfoil was proposed and analyzed. The feasibility of aluminium plate de-icing by the ultrasonic method was achieved. Moreover, the required power density obtained from experiment is up to 10 times less than for conventional thermal de-icing systems. However, the weight and the effectiveness of the ultrasonic system with Langevin-type actuators must be improved. Therefore, the further study could be focused on the following aspects:

- Transducer type and design
- Piezoelectric material selection;
- Acoustic impedance matching, including bond line design

- Possible combination with active and passive de-icing techniques, employment in hybrid de-icing systems;

ACKNOWLEDGMENT

The author would like to thank all co-authors of this paper for their help and support.

References

[1] S. Eger, A. Matveenko. and I. Shatalov. Basis of aviation engineering [Osnovy aviacionnoj tehniki]. 3rd ed., Moskva: Mashinostroenie, 2003, pp.371-380.

[2] F.A. Regulations, Part 25-Airworthiness Standards: Transport Category Airplanes, Federal Aviation Administration (FAA), USA, 2013.

[3] M.B. Bragg, G.M. Gregorek, J.D. Lee, Airfoil aerodynamics in icing conditions, J. Aircr., 23 (1), 1986, pp.76–81.

[4] Y. Cao, Z. Wu, Y. Su, Z. Xu, Aircraft flight characteristics in icing conditions Prog. Aerosp. Sci., 74, 2015, pp.62–80.

[5] F. Lynch, A. Khodadoust. Effects of ice accretions on aircraft aerodynamics. Prog. Aerosp. Sci., 37(8), 2001, pp.669-767.

[6] M. Bragg, A. Broeren, and L. Blumenthal, Iced-airfoil aerodynamics. Prog. Aerosp. Sci., 41(5), 2005, pp.323-362.

[7] T. Strobl, S. Storm, D. Thompson, M. Hornung, F. Thielecke. Feasibility Study of a Hybrid Ice Protection System. J Aircr., 52(6), 2015, pp.2064–2076.

[8] Z. Wang. Recent progress on ultrasonic de-icing technique used for wind power generation, high-voltage transmission line and aircraft. Energy Build., 140, 2017, pp.42–49.

[9] J.L. Palacios, Y. Zhu, E.C. Smith, LJ. Rose. Ultrasonic Shear and Lamb Wave Interface Stress for Helicopter Rotor De-Icing Purposes. 47th AIAA conference, 2006.

[10] J.L. Rose. Ultrasonic guided waves in solid media. 2014.

[11] I.A. Viktorov. Acoustic surface waves in solid bodies [Zvukovyie poverhnostnyie volnyi v tvYordyih telah]. Nauka, 1981.

[12] N. Sonwalkar, S.S. Sunder, S.K. Sharma. Ice/solid adhesion analysis using low-temperature raman microprobe shear apparatus. Appl Spectrosc., 1993.

[13] J.L. Palacios, E. Smith, J.L. Rose. Instantaneous De-Icing of Freezer Ice via Ultrasonic Actuation. AIAA Journal, 49(6), pp.1158-1167.2011;49.